



Possible causes of atherosclerosis: lncRNA *COLCA1* induces oxidative stress in human coronary artery endothelial cells and impairs wound healing

Ming-Peng Li^{1,2,3}, Zi-Chen Hao³, Meng-Qi Yan², Chun-Li Xia², Zhong-Hua Wang³, Ying-Qing Feng^{1,2}

¹The Second School of Clinical Medicine, Southern Medical University, Guangzhou, China; ²Department of Cardiology, Guangdong Cardiovascular Institute, Guangdong Provincial People's Hospital, Guangdong Academy of Medical Sciences, Guangzhou, China; ³Department of Cardiovascular, Chenzhou No. 1 People's Hospital, The First Affiliated Hospital of Xiangnan University, Chenzhou, China

Contributions: (I) Conception and design: ZH Wang, YQ Feng; (II) Administrative support: ZH Wang, YQ Feng; (III) Provision of study materials or patients: ZH Wang, YQ Feng; (IV) Collection and assembly of data: MP Li, ZC Hao, MQ Yan, CL Xia; (V) Data analysis and interpretation: MP Li, ZC Hao, MQ Yan; (VI) Manuscript writing: All authors; (VII) Final approval of manuscript: All authors.

Correspondence to: Zhong-Hua Wang, Chenzhou No. 1 People's Hospital, No. 102 Luojiaying, Chenzhou 423000, China. Email: cyywzh@163.com; Ying-Qing Feng, Guangdong Provincial People's Hospital, No. 106, Zhongshan two Road, Yuexiu District, Guangzhou 510080, China. Email: fyq1819@163.com.

Background: Atherosclerosis is the most common cause of cardiovascular disease, accompanied by high mortality and poor prognosis. Low-density lipoprotein (LDL) and its oxidized form oxidized low-density lipoprotein (oxLDL) play an important role in atherosclerosis. This article will explore the role of the lncRNA *COLCA1* (colorectal cancer associated 1)/*hsa-miR-371a-5p*/*SPP1* (secreted phosphoprotein 1) pathway in oxLDL in causing human coronary artery endothelial cells (HCAECs) inflammation and related biological function changes.

Methods: OxLDL was used to stimulate HCAECs. The inflammatory response and biological function changes of HCAECs were analyzed, total RNA-seq was performed on HCAECs before and after stimulation, and RT-Qpcr (real-time quantitative PCR) was used to verify the differential genes. Interference of the expression of *COLCA1* in HCAECs was performed by siRNA interference technology to verify the role of *COLCA1* in the biological function changes of HCAECs after oxLDL stimulation, and further prove that *COLCA1* affects *SPP1* through *hsa-miR-371a-5p*.

Results: OxLDL can affect the oxidative stress response of HCAECs, which in turn affects the apoptosis and wound healing ability of HCAECs. *COLCA1* and *SPP1* were highly expressed after oxLDL stimulation, while *hsa-miR-371a-5p* was the opposite. After *COLCA1* interference, the oxidative stress level of HCAECs stimulated by oxLDL decreased, the apoptosis level also significantly decreased, and the wound healing ability was enhanced. After simultaneous *COLCA1* interference and recovery of the expression of *hsa-miR-371a-5p*, these improved functions disappeared. The dual-luciferase assay confirmed that *hsa-miR-371a-5p* and *COLCA1*, *hsa-miR-371a-5p* and *SPP1* has binding targets.

Conclusions: OxLDL can up-regulate the expression of *COLCA1* in HCAECs, which in turn affects the intracellular *COLCA1*/*hsa-miR-371a-5p*/*SPP1* pathway to regulate the level of oxidative stress in cells. This in turn affects the level of apoptosis and wound healing ability, which causes cells to produce a continuous inflammatory response.

Keywords: Long non-coding RNA (lncRNA); oxidative stress; wound healing; atherosclerotic plaque; ceRNA

Submitted Jan 07, 2022. Accepted for publication Mar 04, 2022.

doi: 10.21037/atm-22-507

View this article at: <https://dx.doi.org/10.21037/atm-22-507>

Introduction

Atherosclerotic lesions cause coronary atherosclerotic heart disease in the coronary arteries, which causes the vascular lumen to be narrowed or blocked. Therefore, dyslipidemia is a risk factor for coronary heart disease as it is an important cause of atherosclerosis. It has been reported in previous studies (1-3) that diseases caused by a high-fat diet (HFD), such as metabolic syndrome, have an impact on cardiovascular health. Dyslipidemia is related to changes in the physical properties of cell membranes, which may promote reactive oxygen species (ROS) to escape from the mitochondrial electron transport chain or activate nicotinamide adenine dinucleotide phosphate oxidase (NADPH). These processes will increase the production of ROS and increase their tendency to react with other molecules. This leads to oxidation and peroxidation of lipids, proteins, and lipoproteins, and cell membranes are rich in lipids and lipoproteins (4). Peroxidation of the endothelial cell membrane can cause endothelial damage and dysfunction. Low-density lipoprotein cholesterol (LDL-C) and its oxidized form (oxLDL-C) play an essential role in atherosclerosis. Elevated oxLDL-C triggers gene expression of tumor necrosis factor- α (*TNF- α*), especially in blood vessels (5). The enhanced *TNF- α* level increases the permeability of blood vessels to blood macromolecules and causes inflammatory cells to enter the damaged vascular tissue, thereby promoting the formation of atherosclerotic plaques. Therefore, we must further understand how oxLDL causes endothelial cell inflammation and affects the wound healing ability of cells. This will help us better understand the pathogenesis of coronary atherosclerotic heart disease and develop intervention measures.

Long non-coding RNAs (lncRNAs) have been proven to play important regulatory roles in various biological functions of cells. *COLCA1* is a relatively novel lncRNA. It was first studied in colorectal cancer (CRC). Subsequent studies on a variety of cancer prediction models have cited it as a prognostic indicator (6-8), and there are related reports that the abnormal expression of *COLCA1/COLCA2* can cause primary biliary cholangitis (PBC) (9). However, in the study of atherosclerosis, there is no relevant research, and lncRNAs also play a role in the development of atherosclerosis. For example, *PVT1* was found to regulate the *GRB2* gene through *miR-153-3P* to regulate the *ERK/P38* pathway (10). In addition, *PVT1* affects the damage of endothelial cells, and *SNHG12* affects the formation of new blood vessels by modulating the cell cycle of endothelial

cells (11). Therefore, this study investigated the mechanism of *COLCA1* in the development of atherosclerosis.

Secreted phosphoprotein 1 (*SPP1*) is a stromal cell protein, also known as osteopontin (*OPN*), mediating various biological functions (12-14). As a pro-inflammatory cytokine, *SPP1* up-regulates the expression of interferon (*IFN- γ*) and interleukin (*IL-12*) (15,16) and promotes cell-mediated immune responses. In cardiovascular diseases, *SPP1* has a two-sided phenotype in terms of physiology and pathology. The sharp increase in *SPP1* expression has protective functions, such as biomineralization (17,18) and wound healing (19,20). The slow rise of *SPP1* expression indicates the poor prognosis of major adverse cardiovascular events, which is not related to conventional risk factors including myocardial infarction, atherosclerosis, kidney damage, and diabetes.

This study mainly reveals the following mechanism of action: coronary vascular endothelial cells increase the expression of *COLCA1* under the stimulation of oxLDL, and *COLCA1* up-regulates *SPP1* by inhibiting *hsa-miR-371a-5p*, which leads to the continuous inflammation of coronary endothelial cells and the inability to heal wounds. Finally, atherosclerotic plaques are formed. We present the following article in accordance with the MDAR reporting checklist (available at <https://atm.amegroups.com/article/view/10.21037/atm-22-507/rc>).

Methods

Cell lines and reagents

Primary human coronary artery endothelial cells (HCAECs) were provided by Guangzhou Jennio Biotech Co., Ltd. (China). Endothelial Cell Medium (ECM) medium was used for culture.

Cell stimulation and transfection

In this study, oxLDL was used to stimulate HCAECs at a concentration of 50 $\mu\text{g}/\text{mL}$. Additionally, siRNA or an inhibitor was used to transfect HCAECs at a concentration of 100 nM. The transfection reagent used was Lipofectamine 2000 (Life Technologies, USA).

Total RNA-seq analysis

Total RNA was isolated from samples using TRIzol Reagent (Thermo Fisher, # 15596026). Then, 1 μg RNA

and the VAHTS mRNA-seq v2 Library Prep Kit for Illumina (Vazyme Biotech, China) were used for library preparation. Libraries were subjected to deep sequencing with an Illumina HiSeq 3000 at Guangzhou all-perfect Biological Technology Co., Ltd. RNAs (both LncRNA, mRNA, miRNA) with $|\log_2 \text{Ratio}| > 0.6$ and $P < 0.05$ were considered differentially expressed, and differently expressed RNAs (both LncRNA, mRNA, miRNA) were selected to conduct heatmap and hierarchical clustering analyses.

Flow cytometry analysis of apoptosis

In 6-well plates, the processed HCAECs were rinsed in PBS. After trypsinization, the cells were resuspended in binding buffer (100 μL). FITC-conjugated Annexin V and PI (1 μL , Invitrogen, Carlsbad, CA, USA) were added to the binding buffer. After 15 minutes, apoptotic cells were analyzed by flow cytometry (Agilent, USA).

Flow cytometry analysis of ROS

In 6-well plates, the processed HCAECs were rinsed in PBS. After trypsinization, the cells were resuspended in basal medium (1 mL). DCFH-DA probe (2 μL , 10 mM, Guangzhou All-perfect Biological Technology Co., Ltd., China) was added to the basal medium and incubated for 15 minutes at 37 °C and 5% CO_2 . The cells were rinsed 3 times with complete medium. Cells were then analyzed by flow cytometry (Agilent, USA).

Wound healing assay

The processed HCAECs were seeded in 6-well plates (5×10^5 cells/well). At 80% confluence, a 10- μL pipette tip was utilized in the monolayer of cells to generate wounds. Then, cells were washed with PBS, and function of stimulus (genes or oxLDL) on cell migration was assessed after adding medium with 2% FBS. Images were captured to evaluate healing at 0 and 24 hours after wounding.

Luciferase reporter assay

COLCA1 full-length and *SPP1* 3'-UTR of the wild-type (WT) and mutant-type (Mut) *hsa-miR-371a-5p* binding site was generated by Guangzhou All-perfect Biological Technology Co., Ltd. (Guangzhou, China). *COLCA1*-WT/Mut or *SPP1*-WT/Mut was transfected into 293T

cells with *hsa-miR-371a-5p* mimics/NC mimics or *hsa-miR-371-5p* inhibitor/NC inhibitor. Luciferase activity was evaluated by the Dual-Luciferase Reporter Assay (Beyotime Biotechnology, China) after 48 hours of transfection.

Cell proliferation assay

The Cell Counting Kit 8 (CCK-8) (Sigma-Aldrich, USA) was used to assess cell proliferation. The HCAECs of different treatment groups were transferred to 96-well plates and cultured for 12, 24, 36, and 48 hours, and the number of plated cells was 4×10^3 . A total of 20 μL of CCK-8 reagent was added to each well, and the cells were then incubated in a humidified atmosphere of 5% CO_2 for 30 minutes at 37 °C. Then, 100 μL of supernatant was aspirated from each well for analysis. The absorbance of the cell sample at a wavelength of 450 nm was measured with a Sunrise microplate reader (Tecan Group, Ltd., Mannedorf, Switzerland).

Enzyme linked immunosorbent assay (ELISA) detection of inflammatory factors secreted by cells

The cells were plated in a 6-well plate and processed according to groupings. After 48 hours, the cell culture supernatant was collected, centrifuged at 10,000 g at 4 °C for 5 minutes, then the supernatant was obtained. Detection was performed according to the operation of the ELISA detection kit (*IL-6*, E-EL-H6156, *IL-10*, E-EL-H0103c, *IFN- γ* , E-EL-H0108c, Elabscience Biotechnology Co., Ltd.)

Total RNA extraction and real-time quantitative PCR

Total RNA was isolated from the cells using an RNeasy Mini Kit (TIANGEN, China) and then reverse transcribed into cDNA with a MightyScript First Strand cDNA Synthesis Master Mix (GeneCopoeia, USA). The mRNA was detected with All-in-One™ qPCR Mix (GeneCopoeia, USA), and miRNA was detected with All-in-One™ miRNA qRT-PCR Detection Kit (GeneCopoeia, USA) using a fluorescence RT-qPCR system (quantstudio 5, ABI, USA). The primer sequences are shown in *Table 1*.

Statistical analysis

Statistical analyses were performed via GraphPad Prism

Table 1 Sequences of the primers

Name of primer	Sequences of the primers
COLCA1-F	CCCACAGAGAGTCCAGAGAAAC
COLCA1-R	GGGAAGGAGGACAAAATGCTCA
STT3A-AS1-F	GCATGGGGAAAAATAACCTGCC
STT3A-AS1-R	TGTAGGATTCCCCCTGTGTCA
LINC00612-F	CCCCTGATGTACGCCTGTTT
LINC00612-R	CCAACACATGGCTCTGCCTA
ST3GAL5-AS1-F	AGTGAAGCCAGTGAAGTCGG
ST3GAL5-AS1-R	CAGAAGGAGATCACAGGCACA
CYP17A1-AS1-F	TCTGGGGTCAAAGCCAACTAC
CYP17A1-AS1-R	TCTTGCCCTCCATTCTGGCT
hsa-miR-371a-5p-F	ACTCAAAGTGTGGGGGCACT
h-TNFRSF11B-F	GCACCAAAGTAAACGCAGAG
h-TNFRSF11B-R	CTGCTCGAAGGTGAGGTTAG
h-ABCC3-F	TAAGACTTCCCCTCAACATGC
h-ABCC3-R	ATTGCTGGATCCGTTTCAGA
h-SPP1-F	CCGTGGGAAGGACAGTTATG
h-SPP1-R	TAATCTGGACTGCTTGTGGC
h-FTH1-F	GACCCCATTTGTGTGACTT
h-FTH1-R	TATTCCGCCAAGCCAGATTC
H-SLCO2B1-F	TGATCTCCGGCTACCTAAAGA
H-SLCO2B1-R	GCTCACAAACACAATCAAGGC
h-SIK1-F	GGGATGGGAGAGAATCCAGA
h-SIK1-R	AAAGGGGAAGGGGTTTTGTG
h-SLC6A6-F	CTTCATCGCCTTCGTGTGTA
h-SLC6A6-R	GCAACCCACAAAAGGCATAC
h-GCLM-F	CACAGCGAGGAGCTTCAT
h-GCLM-R	CATCTGGAAACTCCCTGACC
h-SLC7A11-F	TTGGCTTCGTCACTACTCTG
h-SLC7A11-R	CTTCTTCTGGTACAACCTCCAGT
h-TNFRSF11B-F	TAAGACTTCCCCTCAACATGC
h-TNFRSF11B-R	ATTGCTGGATCCGTTTCAGA

Software (San Diego, CA, USA), and results were shown as mean \pm SD on the basis of no less than 3 repeats. Student's *t*-test or one-way ANOVA estimated group differences, and statistical significance was set as $P < 0.05$.

Results

OxLDL can alter HCAEC transcriptome expression and biological functions

This study used oxLDL at a concentration of 50 $\mu\text{g}/\text{mL}$ to stimulate HCAECs. By staining with Oil Red O, as shown in *Figure 1A*, obvious lipid droplets were seen in the cells of the oxLDL stimulation group, while there were no obvious lipid droplets in the normal HCAEC group. The results of flow cytometry showed that after oxLDL stimulation, the ROS content in HCAECs increased from $23.62\% \pm 1.37\%$ to $38.16\% \pm 1.04\%$ ($P = 0.001$), and the apoptosis level rose from $14.69\% \pm 1.08\%$ to $25.02\% \pm 1.53\%$ ($P < 0.01$) (*Figure 1B, 1C*). The results of the CCK-8 proliferation assay showed that the proliferation ability of HCAECs was weakened after stimulation (*Figure 1D*). The results of the scratch test showed that the wound healing ability of the cells after stimulation was weakened ($P < 0.01$) (*Figure 1E*). The results of the ELISA assay showed that *IL-6* secretion in the cell culture supernatant was significantly increased after stimulation ($P < 0.01$) (*Figure 1F*). The total RNA-seq results showed that after oxLDL stimulation, the expression of mRNAs, lncRNAs, and miRNAs in HCAECs changed, visualized through heat maps and volcano plots (*Figure 2A-2F*).

The expression of lncRNA COLCA1 increases after oxLDL stimulation and inhibition of lncRNA COLCA1 can reduce the effect of oxLDL on HCAECs

In this experiment, we selected 5 lncRNAs from the sequencing results that have been confirmed to exist and have obvious differences in expression for verification, and we also confirmed that their expression changed after oxLDL stimulation. Among them, the expression difference between *COLCA1* and *LINC00612* was the most significant ($P < 0.001$), which was consistent with the sequencing results (*Figure 3A*). We designed 3 siRNAs for *COLCA1*. The RT-qPCR results showed that hsa-*COLCA1*-si2 had the most obvious interference effect, with an interference efficiency of 90% ($P < 0.01$), while the other siRNAs had no interference effect (*Figure 3B*). Using hsa-*COLCA1*-si2 to transfect HCAECs stimulated by oxLDL, the results showed that after the expression of *COLCA1* was inhibited, the level of apoptosis caused by oxLDL stimulation decreased from $15.99\% \pm 0.9\%$ to $11.28\% \pm 0.55\%$ ($P < 0.01$) and the content of ROS decreased from $35.54\% \pm 0.72\%$ to $26.87\% \pm 0.66\%$ ($P = 0.001$). The cell wound healing ability and proliferation

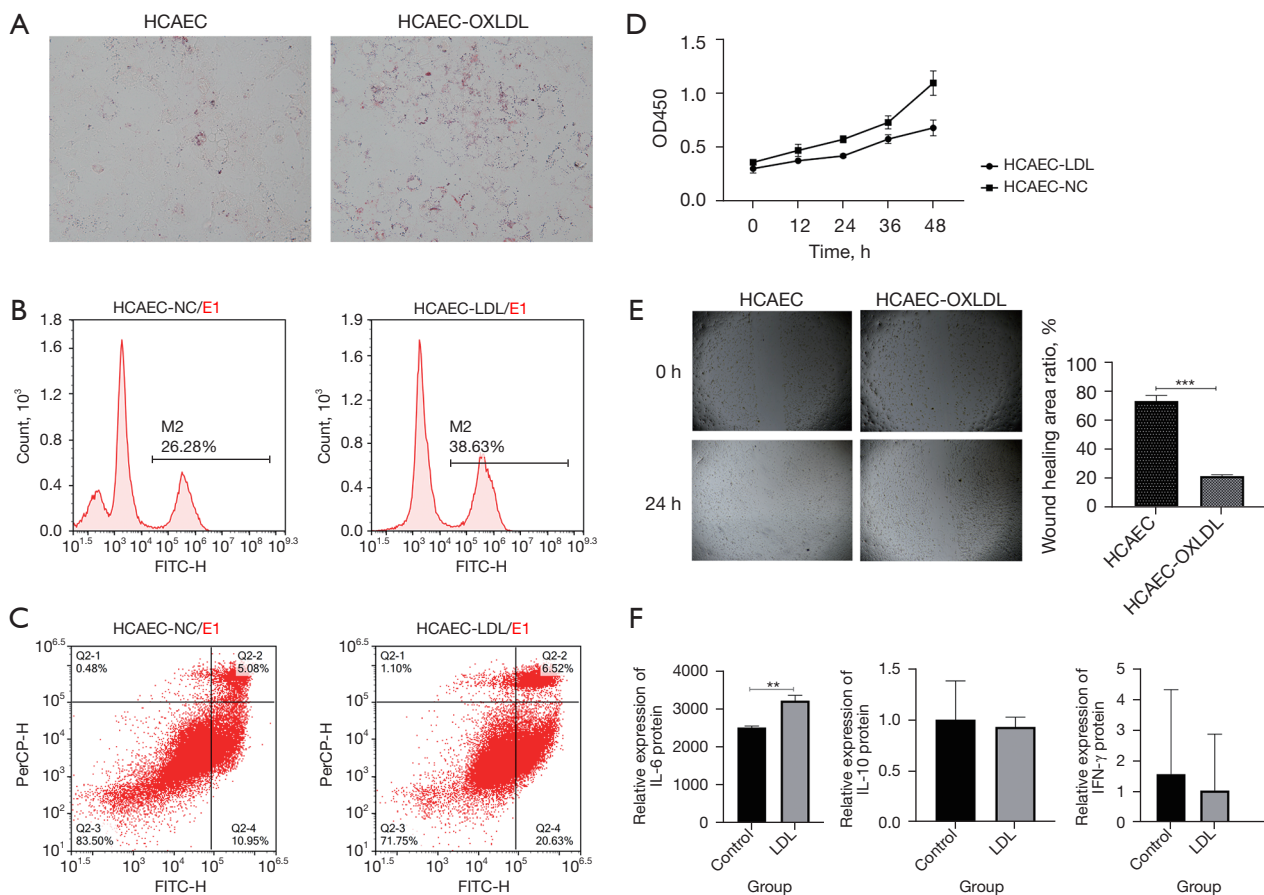


Figure 1 The effect of oxidized low-density lipoprotein (oxLDL) on human coronary artery endothelial cells (HCAECs). (A) Oil Red O staining was used to observe lipid droplets in HCAECs before and after oxLDL stimulation. The stimulation time was 48 hours. The shooting magnification is 40 times. (B) Flow cytometric detection of reactive oxygen species content in HCAECs before and after oxLDL stimulation, and the stimulation time was 48 hours. (C) Flow cytometric detection of apoptosis levels in HCAECs before and after oxLDL stimulation, and the stimulation time was 48 hours. (D) The CCK-8 (Cell Counting Kit-8) assay detected the proliferation level of HCAECs before and after oxLDL stimulation, and the stimulation time was 48 hours. (E) The wound healing assay detected the wound healing ability of HCAECs before and after oxLDL stimulation. The stimulation time was 48 hours, and the detection time was 0–24 hours. The shooting magnification is 40 times. (F) The ELISA (enzyme linked immunosorbent assay) assay detected the secretion of inflammatory factors in HCAECs before and after oxLDL stimulation, and the stimulation time was 48 hours. **, $P < 0.01$; ***, $P < 0.001$.

ability were strengthened ($P < 0.001$). In the absence of oxLDL stimulation, after *COLCA1* inhibition, the wound healing ability of HCAECs was also enhanced ($P < 0.001$), but there was no significant difference in the level of apoptosis and the changes in cellular ROS (Figure 3C–3E).

LncRNA COLCA1 realizes the functional regulation of HCAECs through bsa-miR-371a-5p

By analyzing Starbase prediction results and sequencing results, we found that *bsa-miR-371a-5p* and *COLCA1* have

a binding target. We first performed a dual-luciferase assay to determine that *COLCA1* and *bsa-miR-371a-5p* have a mutual binding target. The *bsa-miR-371a-5p* mimic reduced the ability of the dual-luciferase vector containing the *COLCA1* sequence to express Renilla firefly ($P < 0.001$), and the *bsa-miR-371a-5p* inhibitor the ability of the dual-luciferase vector containing *COLCA1* sequence ($P < 0.05$), and mutations in binding targets, *bsa-miR-371a-5p* mimic, and *bsa-miR-371a-5p* inhibitor did not affect the dual-luciferase vector containing the *COLCA1* sequence (Figure 4A). Next, we used RT-

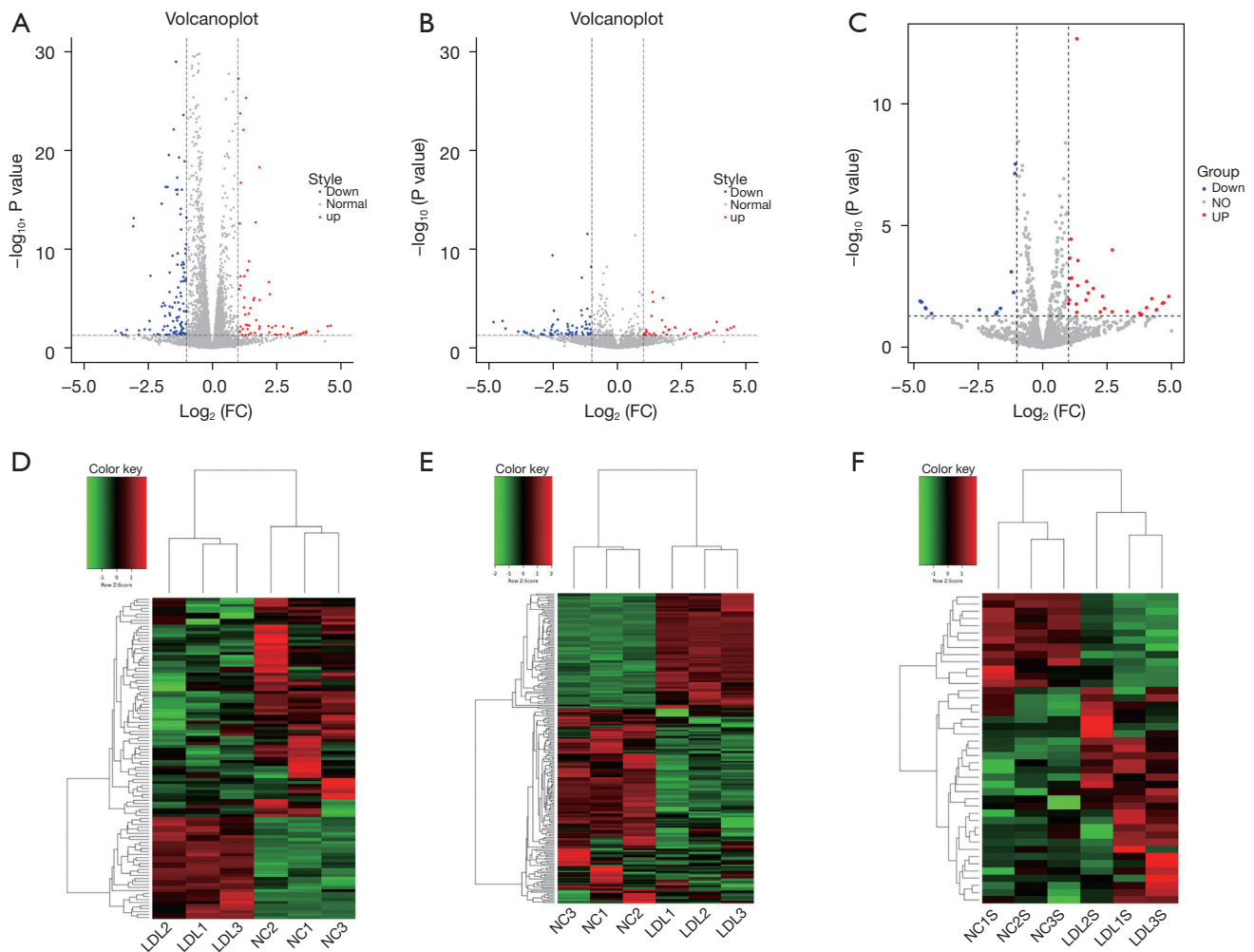


Figure 2 The total RNA-seq results of human coronary artery endothelial cells (HCAECs) before and after oxidized low-density lipoprotein (oxLDL) stimulation. (A) Volcano plot of lncRNA (long non-coding RNA) sequencing data. When the threshold was 2 times and $P < 0.05$, there were 67 up- and 133 down-regulated lncRNAs in HCAECs stimulated by oxLDL compared to normal HCAECs ($n = 3$ biologically independent samples). (B) Volcano plot of mRNA (messenger RNA) sequencing data. When the threshold was 2 times and $P < 0.05$, there were 78 up- and 131 down-regulated mRNAs in HCAECs stimulated by oxLDL compared to normal HCAECs ($n = 3$ biologically independent samples). (C) Volcano plot of miRNA (microRNA) sequencing data. When the threshold was 2 times and $P < 0.05$, there were 30 up- and 13 down-regulated miRNAs in HCAECs stimulated by oxLDL compared to normal HCAECs ($n = 3$ biologically independent samples). (D-F) Hierarchical clustering heat map of total RNA-seq data. Hierarchical clustering shows distinguishable expression profiles of lncRNAs and mRNAs in the normal HCAECs and HCAECs stimulated by oxLDL. Up-regulated expression is indicated in red, and down-regulated expression is indicated in green.

qPCR to detect the expression of *hsa-miR-371a-5p* in HCAECs before and after oxLDL stimulation and found that the expression level of *hsa-miR-371a-5p* decreased after stimulation ($P < 0.001$). In terms of the change in *hsa-miR-371a-5p* after interference with *COLCA1*, the results showed that the expression of *hsa-miR-371a-5p* increased

($P < 0.001$) (Figure 4B,4C). We transfected a mixture of *hsa-COLCA1-si2* and inhibitor NC, *hsa-COLCA1-si2*, and *hsa-miR-371a-5p* inhibitor into oxLDL-stimulated HCAECs and found that *hsa-miR-371a-5p* inhibitor could reverse the cell function improvement effect induced by *hsa-COLCA1-si2*, resulting in deteriorated functioning of

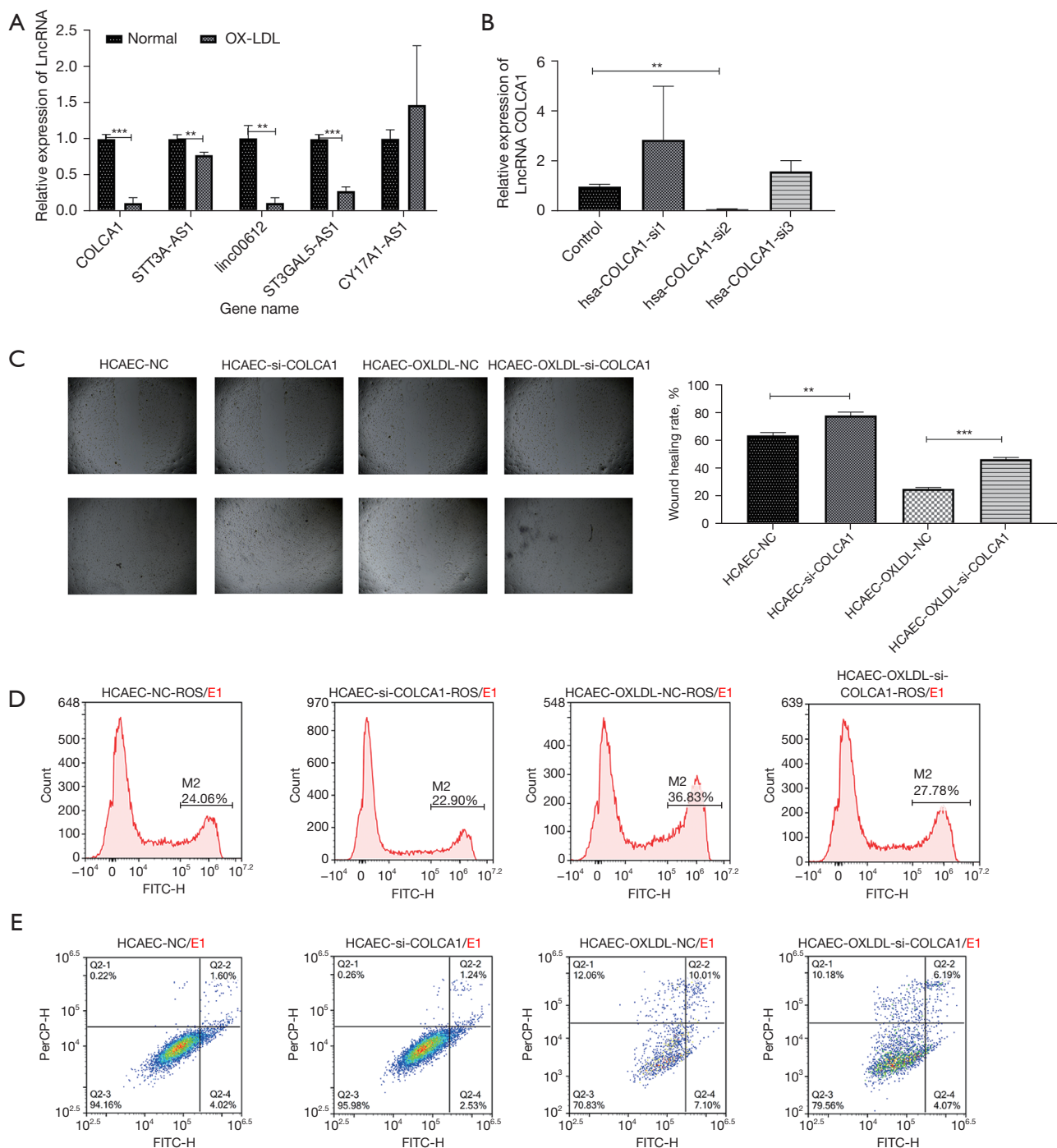


Figure 3 The effect of lncRNA *COLCA1* (colorectal cancer associated 1) on human coronary artery endothelial cells (HCAECs) under different conditions. (A) Real-time quantitative PCR (RT-qPCR) verified the differential expression of lncRNAs in HCAECs before and after oxidized low-density lipoprotein (oxLDL) stimulation. ***, $P \leq 0.001$; **, $P \leq 0.01$. (B) RT-qPCR detected the efficiency of different siRNAs to interfere with the expression of *COLCA1*. **, $P \leq 0.01$. (C) The wound healing assay detected the wound healing ability of HCAECs under different conditions before and after *COLCA1* interference. **, $P \leq 0.01$; ***, $P \leq 0.001$. The shooting magnification is 40 times. (D) Flow cytometric detection of reactive oxygen species content in HCAECs under different conditions before and after *COLCA1* interference. (E) Flow cytometric detection of apoptosis levels in HCAECs under different conditions before and after *COLCA1* interference.

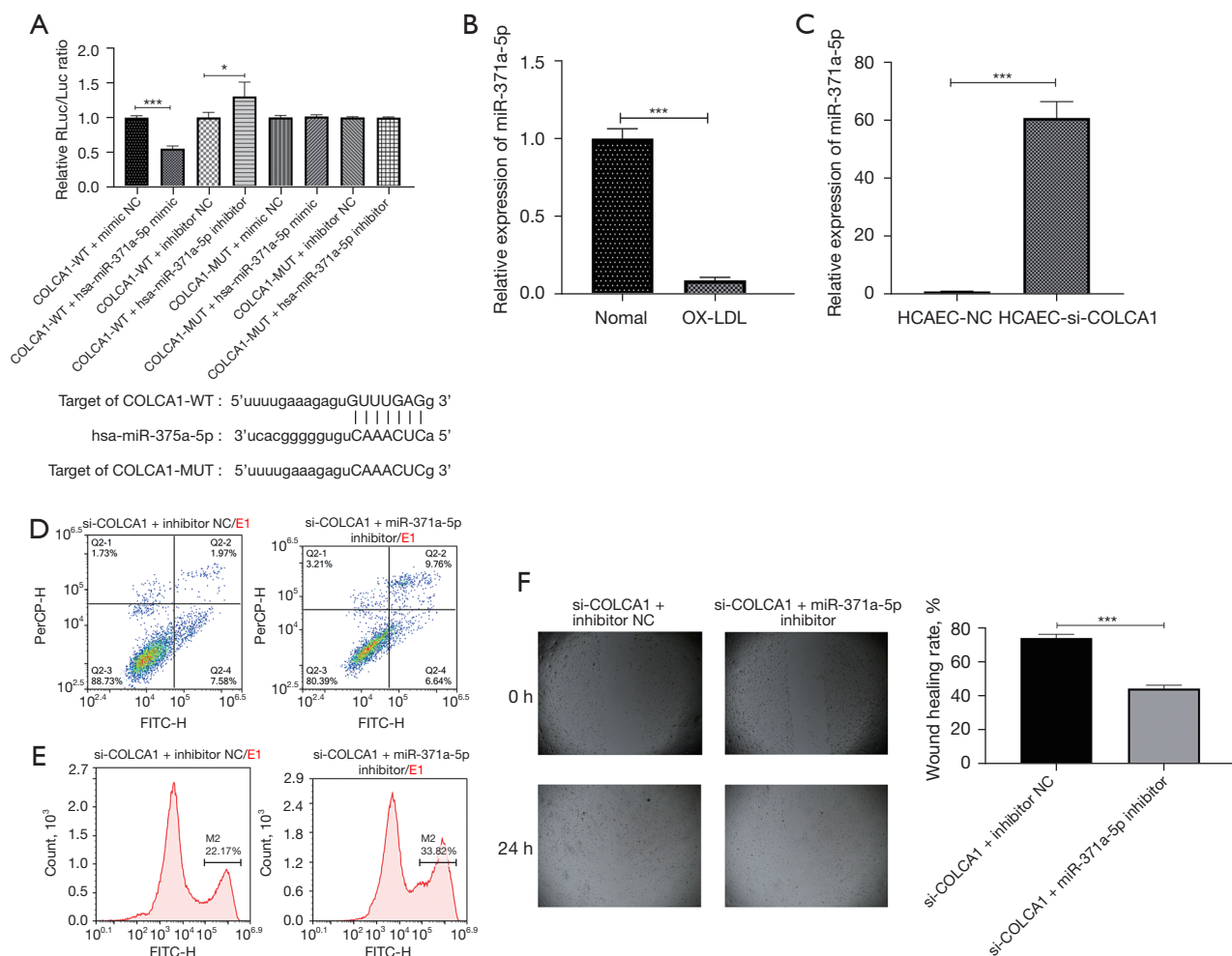


Figure 4 LncRNA *COLCA1* (colorectal cancer associated 1) affects human coronary artery endothelial cells (HCAECs) by regulating hsa-miR-375a-5p. (A) The image above shows the results of a dual luciferase assay verifying the existence of targets for *COLCA1* and hsa-miR-371a-5p, and the image below shows the predicted targets of *COLCA1* and *hsa-miR-371a-5p* and the corresponding mutation sites. ***, $P \leq 0.001$; *, $P < 0.05$. (B) The expression of *hsa-miR-371a-5p* in HCAECs before and after oxidized low-density lipoprotein (oxLDL) stimulation. ***, $P \leq 0.001$. (C) The *hsa-miR-371a-5p* expression of HCAECs before and after *COLCA1* interference. ***, $P \leq 0.001$. (D) After oxLDL stimulation and *COLCA1* interference, the apoptosis level of HCAECs before and after the recovery of *hsa-miR-371a-5p* expression. The stimulation time was 48 hours. (E) After oxLDL stimulation and *COLCA1* interference, the reactive oxygen species content of HCAECs before and after the recovery of *hsa-miR-371a-5p* expression. The stimulation time was 48 hours. (F) After oxLDL stimulation and *COLCA1* interference, the wound healing ability of HCAECs before and after *hsa-miR-371a-5p* expression was restored, and the stimulation time was 24 hours. ***, $P \leq 0.001$. The shooting magnification is 40 times.

HCAECs. As shown in *Figure 4D-4F*, compared with the hsa-*COLCA1*-si2 group, the apoptosis level of the hsa-*COLCA1*-si2 + *hsa-miR-371a-5p* inhibitor group increased from $10\% \pm 0.5\%$ to $15.61\% \pm 0.99\%$ ($P = 0.006$) and ROS increased from $21.1\% \pm 2.2\%$ to $30.87\% \pm 1.5\%$ ($P < 0.05$). The cell proliferation and wound healing abilities were significantly.

SPP1 is the target gene of *hsa-miR-371a-5p*

We combined the sequencing results and results from TargetScan, Starbase, and other databases to predict the target genes of *hsa-miR-371a-5p* and found 8 potential target genes. We previously found that the expression of *hsa-miR-371a-5p* increases after *COLCA1* interference.

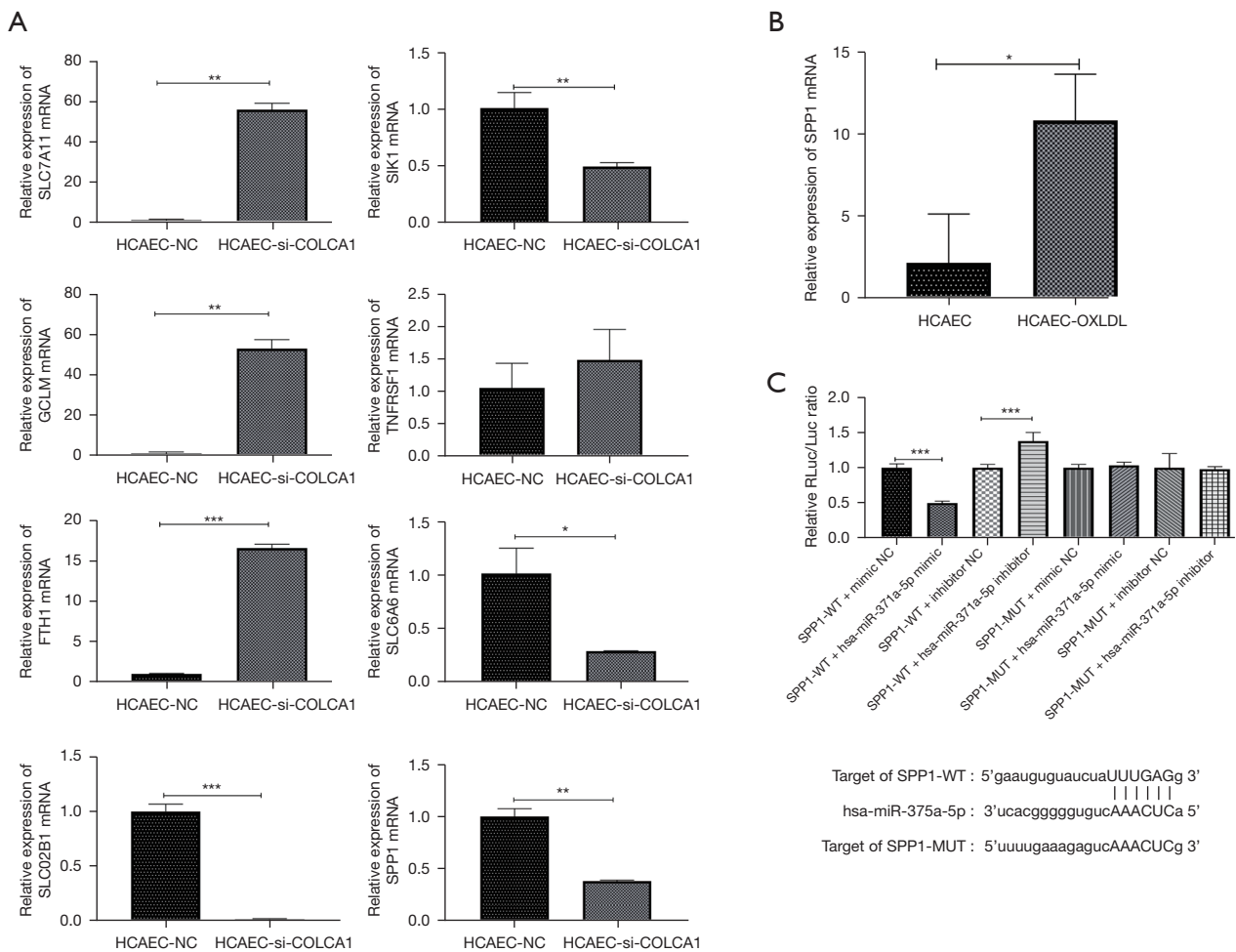


Figure 5 The target gene of *hsa-miR-371a-5p* is *SPP1* (secreted phosphoprotein 1). (A) The real-time quantitative PCR (RT-qPCR) experiment verified the potential target genes of the *COLCA1/miR-371a-5p* axis. ***, $P \leq 0.001$; **, $P \leq 0.01$; *, $P < 0.05$. (B) The RT-qPCR detection of *SPP1* expression in human coronary artery endothelial cells (HCAECs) before and after oxidized low-density lipoprotein (oxLDL) stimulation. *, $P < 0.05$. (C) The image above shows the results of a dual luciferase assay verifying the existence of targets for *SPP1* and *hsa-miR-371a-5p*, and the image below shows the predicted targets of *SPP1* and *hsa-miR-371a-5p* and the corresponding mutation sites. ***, $P \leq 0.001$.

On this basis, we tested these 8 target genes and found that *SPP1*, *SIK1*, *SLC6A6*, and *SLC02B1* decreased after *COLCA1* interference (Figure 5A). We then performed RT-qPCR detection on normal HCAECs and oxLDL-stimulated HCAECs, and the expression of *SPP1* was found to have increased (Figure 5B). We also conducted a dual-luciferase assay and found that *hsa-miR-371a-5p* mimic and inhibitor can regulate the fluorescent expression ability of the dual-luciferase vector containing the 3'UTR region of *SPP1* but not the dual-luciferase vector containing the mutated predicted target (Figure 5C).

Discussion

OxLDL can stimulate endothelial cells to produce an inflammatory response (21-23). In this study, under the stimulation of an oxLDL concentration of 50 $\mu\text{g/mL}$, endothelial cells experienced oxidative stress, and the content of ROS increased. In addition, the level of cell apoptosis rose, the secretion of inflammatory factors increased, and the wound healing ability was weakened. All these findings show that our atherosclerosis cell model is credible.

For a long time, proteins have been regarded as the center of the gene regulation network. However, only 2% of RNAs

in the mammalian transcriptome encode proteins (24), while the majority of the human transcriptome comprises non-coding RNAs, including lncRNAs. Furthermore, the expression of ncRNAs in different tissues is more specific than that of protein-coding genes, indicating that the function of lncRNAs is closely related to the functional specificity of the tissue (25). Therefore, lncRNAs may represent important regulatory factors for heart development and disease processes, and may be new disease biomarkers or therapeutic targets for cardiovascular diseases and their risk factors. We performed total RNA-seq on HCAECs before and after stimulation with oxLDL. From the cluster diagram, it can be seen that the samples in the same group have good reproducibility. Therefore, the results have high reliability. The sequencing results obtained differentially expressed lncRNAs, mRNAs, and miRNAs. Among them, there were both known genes and unknown predictive genes. In this study, the known genes were investigated, and finally lncRNA *COLCA1* was selected for follow-up research. *COLCA1* and *COLCA2* were initially identified by Peltekova *et al.* as genes whose expression levels are significantly related to CRC susceptibility SNPs, and were subsequently confirmed by Hitomi *et al.* to be associated with PBC susceptibility (26,27). Our research confirms that *COLCA1* is also related to inflammation in cardiovascular diseases. *COLCA1* causes the continuous inflammation of HCAECs. On the one hand, this leads to an increase in the apoptosis of HCAECs, while on the other hand, it also leads to the deterioration of the wound healing ability of HCAECs. This may form a reciprocal feedback loop. Inflammation causes failure in wound healing, and the unhealed wound leads to surrounding inflammation so that atherosclerotic plaques are gradually formed.

In recent years, long noncoding RNAs (lncRNAs) have been involved in many physiological and pathological processes in the heart. Recent studies have shown that lncRNAs are dynamically expressed in cardiovascular disease and involved in regulation through multiple molecular mechanisms and have become a key part of epigenetic and transcriptional regulatory pathways in cardiac development and the occurrence and progression of myocardial infarction (28-30). lncRNAs regulate gene expression at the transcription and post-transcriptional levels. Complementary sites on lncRNAs enable them to recognize and bind to mRNAs, miRNAs, or other lncRNAs and perform highly specific regulation. Protein binding sites interact with proteins to produce various ribonucleoprotein particles with different biological functions (31). At present, the Relatively

well-studied mechanism is that lncRNA acts as a competitive endogenous RNA (ceRNA), which adsorbs the target miRNA and makes the miRNA unable to function. Through the results of total RNA-seq and bioinformatics analysis, we discovered the potential target of *COLCA-hsa-miR-371a-5p* and verified it through a dual luciferase assay. *hsa-miR-371a-5p* is the hsa-miR-371a encoded by chromosome 19, further cleaved by Dicer ribonuclease. There are few studies on *hsa-miR-371a-5p*, and they are mainly focused on tumors and inflammation-related studies. Ernst *et al.*'s research showed that the miRNA microarray results changed significantly in term and preterm placentas, among which *hsa-miR-371a-5p* showed significant changes (32). However, Jang *et al.* used RT-qPCR to verify the samples (both term and preterm placentas) in large quantities and found that *hsa-miR-371a-5p* did not change significantly, while *hsa-miR-371a-5p* was confirmed to be able to regulate the inflammatory target gene LEF1 found in the samples (33). Tang *et al.* found that *hsa-miR-371a-5p* is significantly under-expressed in induced pluripotent stem cells (iPSCs) derived from systemic lupus erythematosus (SLE) and may cause significantly high expression of AK4, thereby promoting the development of SLE. The above studies show that *hsa-miR-371a-5p* may have some relationship with the occurrence and development of inflammation (34). We also found that *hsa-miR-371a-5p* had significantly lower expression in HCAECs stimulated by oxLDL, and inhibiting the expression of *COLCA1* could restore the high expression of *hsa-miR-371a-5p* and improve the physiology of HCAEC functioning, which further proves the relationship between *hsa-miR-371a-5p* and the development of inflammation. Therefore, *hsa-miR-371a-5p* should be a potential factor that can effectively inhibit inflammation. However, in atherosclerosis, it is inhibited by *COLCA1* and cannot play a role.

The most common mechanism of action of miRNAs is to bind to the 3'UTR region of mRNAs so that the mRNA is degraded or cannot be transcribed. A large number of experiments have confirmed this mechanism. This study also used this mechanism to predict and verify the target genes that *hsa-miR-371a-5p* acts on. Through database prediction and dual-luciferase assay verification, we confirmed that *hsa-miR-371a-5p* targets *SPP1*. *SPP1* is a gene that has been identified to be associated with vascular diseases and can up-regulate the expression of IFN- γ and IL-12. Barchetta *et al.* confirmed that higher *SPP1* is associated with insulin resistance, atherosclerosis, and coronary heart disease (35). Chellan *et al.* demonstrated that LDL could significantly increase the expression of *SPP1* in vascular smooth muscle

cells (VSMCs) (36). VSMCs are core participants in the development of carotid atherosclerotic plaques. Goikuria *et al.* found that *SPP1* was significantly increased in VSMCs in atherosclerotic plaques (37). The above research results are consistent with our experimental results, and we can conclude that *SPP1* is indeed an important gene related to the formation of atherosclerotic plaques. This is mainly due to the abnormal expression of *hsa-miR-371a-5p*, leading to dysregulated expression of *SPP1*, which then stimulates cells to secrete inflammatory factors so that inflammation continuously occurs.

In summary, we analyzed the total RNA-seq results of HCAECs before and after oxLDL stimulation. We obtained an lncRNA, *COLCA1*, that has not been studied in cardiovascular disease and confirmed that *COLCA1* could cause the continuous occurrence of cardiovascular disease inflammation, which in turn leads to atherosclerosis and the formation of hardened plaques. *COLCA1* completes this regulation process through the *hsa-miR-371a-5p/SPP1* axis. Therefore, in follow-up studies, *hsa-miR-371a-5p* may be used as a potential factor for treating atherosclerotic plaques. Compared with lncRNA or mRNA, miRNA is relatively stable *in vivo* because of its small number of bases and is regarded as a more reliable detection index in clinical detection. Can we detect whether *hsa-miR-371a-5p* expression to judge the effect of treatment in patients. The *hsa-miR-371a-5p* agonist can be delivered into the blood vessels by targeting nanomaterials or combined with statins to control the inflammation of the patient's vascular endothelial cells, thereby reducing the inflammation of the inflammation the patient's condition, which is also a direction for our follow-up research.

Acknowledgments

Funding: This work was supported by the scientific research plan project of Hunan Provincial Health Commission (No. 202203012553); Scientific and Technological Development Program of Chenzhou Science and Technology Bureau (No. zdyf201927).

Footnote

Reporting Checklist: The authors have completed the MDAR reporting checklist. Available at <https://atm.amegroups.com/article/view/10.21037/atm-22-507/rc>

Data Sharing Statement: Available at <https://atm.amegroups.com/article/view/10.21037/atm-22-507/dss>

[com/article/view/10.21037/atm-22-507/dss](https://atm.amegroups.com/article/view/10.21037/atm-22-507/dss)

Conflicts of Interest: All authors have completed the ICMJE uniform disclosure form (available at <https://atm.amegroups.com/article/view/10.21037/atm-22-507/coif>). The authors have no conflicts of interest to declare.

Ethical Statement: The authors are accountable for all aspects of the work in ensuring that questions related to the accuracy or integrity of any part of the work are appropriately investigated and resolved.

Open Access Statement: This is an Open Access article distributed in accordance with the Creative Commons Attribution-NonCommercial-NoDerivs 4.0 International License (CC BY-NC-ND 4.0), which permits the non-commercial replication and distribution of the article with the strict proviso that no changes or edits are made and the original work is properly cited (including links to both the formal publication through the relevant DOI and the license). See: <https://creativecommons.org/licenses/by-nc-nd/4.0/>.

References

1. Wali JA, Jarzebska N, Raubenheimer D, et al. Cardio-Metabolic Effects of High-Fat Diets and Their Underlying Mechanisms-A Narrative Review. *Nutrients* 2020;12:1505.
2. Wei F, Liu Y, Bi C, et al. Nostoc sphaeroids Kütz powder ameliorates diet-induced hyperlipidemia in C57BL/6j mice. *Food Nutr Res* 2019. doi: 10.29219/fnr.v63.3618.
3. Li N, Cheng W, Huang T, et al. Vascular Adventitia Calcification and Its Underlying Mechanism. *PLoS One* 2015;10:e0132506.
4. Abbasnezhad A, Niazmand S, Mahmoudabady M, et al. Nigella sativa L. seed regulated eNOS, VCAM-1 and LOX-1 genes expression and improved vasoreactivity in aorta of diabetic rat. *J Ethnopharmacol* 2019;228:142-7.
5. Niemann-Jönsson A, Dimayuga P, Jovinge S, et al. Accumulation of LDL in rat arteries is associated with activation of tumor necrosis factor- α expression. *Arterioscler Thromb Vasc Biol* 2000;20:2205-11.
6. Zheng J, Zhao Z, Wan J, et al. N-6 methylation-related lncRNA is potential signature in lung adenocarcinoma and influences tumor microenvironment. *J Clin Lab Anal* 2021;35:e23951.
7. Qi-Dong X, Yang X, Lu JL, et al. Development and Validation of a Nine-Redox-Related Long Noncoding RNA Signature in Renal Clear Cell Carcinoma. *Oxid Med*

- Cell Longev 2020;2020:6634247.
8. Song N, Kim K, Shin A, et al. Colorectal cancer susceptibility loci and influence on survival. *Genes Chromosomes Cancer* 2018;57:630-7.
 9. Harris M. Helping the person with an altered self-image. *Geriatr Nurs* 1986;7:90-2.
 10. Guo J, Li J, Zhang J, et al. LncRNA PVT1 knockdown alleviated ox-LDL-induced vascular endothelial cell injury and atherosclerosis by miR-153-3p/GRB2 axis via ERK/p38 pathway. *Nutr Metab Cardiovasc Dis* 2021;31:3508-21.
 11. Gross DA, Cheng HS, Zhuang R, et al. Deficiency of lncRNA SNHG12 impairs ischemic limb neovascularization by altering an endothelial cell cycle pathway. *JCI Insight* 2022;7:150761.
 12. Lok ZSY, Lyle AN. Osteopontin in Vascular Disease. *Arterioscler Thromb Vasc Biol* 2019;39:613-22.
 13. Abdelaziz Mohamed I, Gadeau AP, Hasan A, et al. Osteopontin: A Promising Therapeutic Target in Cardiac Fibrosis. *Cells* 2019;8:1558.
 14. Waller AH, Sanchez-Ross M, Kaluski E, et al. Osteopontin in cardiovascular disease: a potential therapeutic target. *Cardiol Rev* 2010;18:125-31.
 15. Maeno Y, Nakazawa S, Yamamoto N, et al. Osteopontin participates in Th1-mediated host resistance against nonlethal malaria parasite *Plasmodium chabaudi chabaudi* infection in mice. *Infect Immun* 2006;74:2423-7.
 16. Renkl AC, Wussler J, Ahrens T, et al. Osteopontin functionally activates dendritic cells and induces their differentiation toward a Th1-polarizing phenotype. *Blood* 2005;106:946-55.
 17. Cho HJ, Cho HJ, Kim HS. Osteopontin: a multifunctional protein at the crossroads of inflammation, atherosclerosis, and vascular calcification. *Curr Atheroscler Rep* 2009;11:206-13.
 18. Si J, Wang C, Zhang D, et al. Osteopontin in Bone Metabolism and Bone Diseases. *Med Sci Monit* 2020;26:e919159.
 19. Shirakawa K, Endo J, Kataoka M, et al. IL (Interleukin)-10-STAT3-Galectin-3 Axis Is Essential for Osteopontin-Producing Reparative Macrophage Polarization After Myocardial Infarction. *Circulation* 2018;138:2021-35.
 20. Weber CE, Li NY, Wai PY, et al. Epithelial-mesenchymal transition, TGF- β , and osteopontin in wound healing and tissue remodeling after injury. *J Burn Care Res* 2012;33:311-8.
 21. Peng K, Jiang P, Du Y, et al. Oxidized low-density lipoprotein accelerates the injury of endothelial cells via circ-USP36/miR-98-5p/VCAM1 axis. *IUBMB Life* 2021;73:177-87.
 22. Chang TT, Yang HY, Chen C, et al. CCL4 Inhibition in Atherosclerosis: Effects on Plaque Stability, Endothelial Cell Adhesiveness, and Macrophages Activation. *Int J Mol Sci* 2020;21:6567.
 23. Zeng Y, Xu J, Hua YQ, et al. MDM2 contributes to oxidized low-density lipoprotein-induced inflammation through modulation of mitochondrial damage in endothelial cells. *Atherosclerosis* 2020;305:1-9.
 24. Shabalina SA, Spiridonov NA. The mammalian transcriptome and the function of non-coding DNA sequences. *Genome Biol* 2004;5:105.
 25. Ransohoff JD, Wei Y, Khavari PA. The functions and unique features of long intergenic non-coding RNA. *Nat Rev Mol Cell Biol* 2018;19:143-57.
 26. Peltekova VD, Lemire M, Qazi AM, et al. Identification of genes expressed by immune cells of the colon that are regulated by colorectal cancer-associated variants. *Int J Cancer* 2014;134:2330-41.
 27. Hitomi Y, Aiba Y, Kawai Y, et al. rs1944919 on chromosome 11q23.1 and its effector genes COLCA1/ COLCA2 confer susceptibility to primary biliary cholangitis. *Sci Rep* 2021;11:4557.
 28. Jaé N, Dimmeler S. Noncoding RNAs in Vascular Diseases. *Circ Res* 2020;126:1127-45.
 29. Gomes CPC, Schroen B, Kuster GM, et al. Regulatory RNAs in Heart Failure. *Circulation* 2020;141:313-28.
 30. Babapoor-Farrokhran S, Gill D, Rasekhi RT. The role of long noncoding RNAs in atrial fibrillation. *Heart Rhythm* 2020;17:1043-9.
 31. Thum T, Condorelli G. Long noncoding RNAs and microRNAs in cardiovascular pathophysiology. *Circ Res* 2015;116:751-62.
 32. Ernst S, Heinzlmann J, Bohle RM, et al. The metastatic potential of seminomatous germ cell tumours is associated with a specific microRNA pattern. *Andrology* 2020;8:1687-98.
 33. Jang HY, Lim SM, Lee HJ, et al. Identification of microRNAs and their target genes in the placenta as biomarkers of inflammation. *Clin Exp Reprod Med* 2020;47:42-53.
 34. Tang D, Chen Y, He H, et al. Integrated analysis of mRNA, microRNA and protein in systemic lupus erythematosus-specific induced pluripotent stem cells from urine. *BMC Genomics* 2016;17:488.
 35. Barchetta I, Ceccarelli V, Cimini FA, et al. Impaired bone matrix glycoprotein pattern is associated with increased cardio-metabolic risk profile in patients with type 2

diabetes mellitus. *J Endocrinol Invest* 2019;42:513-20.

36. Chellan B, Rojas E, Zhang C, et al. Enzyme-modified non-oxidized LDL (ELDL) induces human coronary artery smooth muscle cell transformation to a migratory and osteoblast-like phenotype. *Sci Rep* 2018;8:11954.

37. Goikuria H, Freijo MDM, Vega Manrique R, et al. Characterization of Carotid Smooth Muscle Cells during Phenotypic Transition. *Cells* 2018;7:23.

(English Language Editor: C. Betlazar-Maseh)

Cite this article as: Li MP, Hao ZC, Yan MQ, Xia CL, Wang ZH, Feng YQ. Possible causes of atherosclerosis: lncRNA *COLCA1* induces oxidative stress in human coronary artery endothelial cells and impairs wound healing. *Ann Transl Med* 2022;10(6):286. doi: 10.21037/atm-22-507